Human iPSC-derived Committed Cardiac Progenitors Generate Cardiac Tissue Grafts in a Swine Ischemic Cardiomyopathy Model without Triggering Ventricular Arrhythmias

Amish N. Raval, MD[1,2]*, Eric G. Schmuck, PhD[1], Vladislav Leonov, PhD[1], Sushmita Roy, PhD[1], Yukihiro Saito, MD, PhD[1], Tianhua Zhou, MD[1], Hae Jae Jang, BS[1], Kaylee Wilker, BS[1], James Conklin, BS[2], Timothy A. Hacker, PhD[3], Chad Koonce, BS[4], Meghan Boyer, BS[4], Kristin Stack, BS[4], Ellen Hebron, BS[4], Scott K. Nagle, MD, PhD[5], Jianhua Zhang, PhD[1], Patrick C.H. Hsieh, MD, PhD[1,6,7], Timothy J. Kamp, MD, PhD[1,6]*

[1]Department of Medicine, Division of Cardiovascular Medicine, University of Wisconsin School of Medicine and Public Health, Madison, WI, USA.

[2]Department of Biomedical Engineering, University of Wisconsin, Madison, USA

[3]Cardiovascular Research Center, University of Wisconsin-Madison School of Medicine and Public Health, Madison, USA

[4]Fujifilm Cellular Dynamics Inc., Madison, WI, USA

[5]Department of Radiology, University of Wisconsin School of Medicine and Public Health, Madison, WI, USA

[6]Department of Cell and Regenerative Biology, University of Wisconsin-Madison, USA

[7]Institute of Biomedical Sciences, Academia Sinica, Taipei, Taiwan.

*To whom correspondence should be addressed:

Timothy J. Kamp, tjk@medicine.wisc.edu, 1111 Highland Ave., WIMR II 8459, Madison, WI 53705

Amish N Raval, anr@medicine.wisc.edu, H4/568, Box 3248 Clinical Science Center, 600 Highland Ave., Madison, WI 53792

Short Title: Committed Cardiac Progenitors for Cardiac Repair

Word Count: 8607

Journal Subject Terms: Cell Therapy, Stem cells, Heart Failure, Chronic Ischemic Heart Disease, Treatment.

ABSTRACT

Background: Intramyocardial injection of human pluripotent stem cell-derived cardiomyocytes following a myocardial infarction (MI) improves cardiac function in large animal models, but associated ventricular arrhythmias are major safety concern. We hypothesized that transendocardial injection of human induced pluripotent stem cell (hiPSC)-derived committed cardiac progenitor cells (CCPs), combined with cardiac fibroblast-derived extracellular matrix (cECM) to enhance cell retention, will generate cardiac tissue grafts improving contractility without triggering ventricular arrhythmias.

Methods: hiPSCs were differentiated using bioreactors and small molecules to produce committed cardiac progenitor cells (CCPs). MI was created using a coronary artery balloon occlusion and reperfusion model in Yucatan mini pigs. Four weeks later, epicardial needle injections of CCPs+cECM were performed in a small initial feasibility cohort (n=6), and then transendocardial injections of CCPs+cECM (n=14), CCPs alone (n=14), cECM alone (n=4) or vehicle control (n=13) into the peri-infarct region in a randomized cohort. Arrhythmias were evaluated using implanted event recorders. Magnetic resonance imaging (MRI) and invasive pressure-volume assessment were used to evaluate left ventricular anatomic and functional performance. Detailed histology was performed to detect and characterize human grafts.

Results: A scalable biomanufacturing protocol was developed generating CCPs which can efficiently differentiate into cardiomyocytes or endothelial cells in vitro. Intramyocardial delivery of CCPs to post-MI porcine hearts resulted in engraftment and differentiation of CCPs to form ventricular cardiomyocyte rich grafts. There was no significant difference in cardiac MRI-based measured cardiac volumes or function

between control, CCP and CCP+cECM groups; however, pressure-volume analysis showed an improvement in dobutamine-stimulated functional reserve in CCP and CCP+cECM groups. Delivery of CCPs did not result in tumors or ventricular arrhythmias.

Conclusions: Transendocardial delivery of CCPs with or without cECM into post-MI porcine hearts resulted in comparable human cardiomyocyte grafts which did not improve resting LV function but did improve stress-induced contractile reserve without triggering ventricular arrhythmias.

Key words: Stem Cell, Heart Failure, Treatment, Trial, Catheter

INTRODUCTION

Currently approved medication and device therapies can blunt the progression of heart failure (HF) following myocardial infarction (MI), but the morbidity and mortality in post - MI survivors remain significant.[1,2] For patients who suffer large MIs, replacement of necrotic myocardium with fibrotic scar frequently leads to progressive heart failure, and there are currently no available treatments to replace lost cardiomyocytes and restore contractility. Therefore, cell-based therapies have been investigated for their potential to generate functional cardiac tissue in post-MI or ischemic cardiomyopathy animal models and patients. More than two decades of investigations and clinical trials with a variety of adult cell sources such as bone marrow mononuclear cells have produced no clear evidence of new functional heart muscle or consistent improvements in clinical outcomes.[3] In contrast, post-MI delivery of human pluripotent stem cell (PSC)-derived cardiomyocytes (CMs) from embryonic stem cells (ESCs) or induced pluripotent stem cells (iPSCs) has produced viable cardiomyocyte grafts in rat,[4-7] guinea pig,[8-10] swine,[11-14] and non-human primate[15-17] myocardium. However, large animal experimental studies using hPSC-CMs have been complicated by ventricular arrhythmias, relatively low cell retention in the myocardium and mixed functional results.

hPSC-derived cardiac progenitor cells are also being investigated for cardiac cell therapy in the post-MI failing heart,[18,19] but progenitor cells are a less studied cell preparation for therapy relative to hPSC-CMs. However, there are several features that make cardiac progenitors cells a promising cell source. Cardiac progenitor cells are smaller cells than hPSC-CMs and may be more amenable to manipulation and cell delivery while maintaining viability. The hPSC-derived cardiac progenitor cells are proliferative and therefore may generate larger hPSC-CM grafts per cell delivered. Importantly, cardiac

88 progenitor cells can differentiate to not only hPSC-CMs but also other cardiac cell
89 lineages such as endothelial cells and smooth muscle cells needed to generate viable
90 cardiac tissue grafts. The first in human heart failure treatment clinical trial using hPSCs
91 tested early stage hESC-derived progenitors delivered in a fibrin patch at the time of
92 coronary artery bypass surgery and demonstrated safety for this preparation.[18] However,
93 hPSCs undergo a dynamic range of cell state transitions in the process of differentiating
94 to terminal cardiac lineages which are variably referred to as cardiac progenitors, and the
95 specific characteristics of the given progenitor state chosen for cell therapy is critically
96 important. The optimal cardiac progenitor cell population isolated from differentiating
97 hPSCs and delivery strategy for cardiac repair remain to been determined.

98 Low cell retention is a vexing problem for all cardiac cell therapies. Our group previously
99 described a cardiac extracellular matrix (cECM) engineered biomaterial using high-
100 density culture-expanded cardiac fibroblasts isolated from human cadaveric hearts.
101 cECM is an acellular, uniquely fibronectin abundant, non-chemically cross-linked, non-
102 hydrogel scaffold with immunomodulatory and angiogenic properties that can be
103 formulated into particulates, reconstituted into solution, and administered as an
104 injectable[20,21]. cECM was shown to educate monocytes to a distinct population of
105 macrophages that exhibit anti-inflammatory and pro-angiogenic features,[21] and can
106 promote myocardial retention of mesenchymal stem cells in rodent heart disease models
107 when co-delivered epicardially via an open chest.[22,23] In comparison, a more clinically
108 appealing delivery approach is transendocardial injection (TEI). TEI uses a steerable,
109 needle tipped catheter that is introduced into the left ventricle via a femoral artery to
110 perform targeted intramuscular injections from the endocardial surface.

111 In this study, we tested whether human iPSC-derived committed cardiac progenitors
112 (CCPs) alone or with cECM could be safely delivered to post-MI failing porcine heart and
113 engraft to form cardiac tissue grafts that lead to improvements in functional outcomes.
114 We observed that the CCPs, regardless of the presence of cECM, successfully engrafted
115 and differentiated into cardiomyocytes, endothelial cells and fibroblasts, leading to the
116 formation of cardiac tissue grafts. Cardiac MRI did not show significant improvement in
117 chamber size or ejection fraction, but pressure-volume analysis demonstrated an
118 improvement in dobutamine-stimulated functional reserve by CCPs. Cell delivery did not
119 induce ventricular arrhythmias in the engrafted hearts.

120 **METHODS**

121 For detailed methods, please see the Supplemental Methods section in the Supplemental
122 Material. Data and study materials are available from the corresponding authors upon
123 reasonable request. All animal use in this study adhered to an approved protocol by the
124 institutional animal care and use committee at the University of Wisconsin – Madison,
125 protocol, M005512-R03-A01.

126 Statistical Analysis

127 Statistical analysis was carried out using GraphPad Prism version 9. MRI data was
128 analyzed with a 2-way ANOVA with a Sidak post-hoc analysis for multiple comparisons.
129 Pressure volume loops were analyzed with a One-Way ANOVA with a Bonferroni post-
130 hoc analysis. All data presented as mean +/- standard error of the mean unless
131 otherwise stated as standard deviation. Statistical significance was defined as $P<0.05$.

132 **RESULTS**

133 Production of human iPSC-derived CCPs

134 For scalable production of human iPSC-derived CCPs, iPSCs were propagated as
135 monolayer cultures in CELLSTACK culture chambers. Cells were singularized and
136 inoculated into PBS3 Bioreactors to form cellular aggregates that were differentiated in
137 suspension culture using an accelerated small molecule-based protocol employing
138 biphasic modulation of Wnt signaling along with application of a rho-kinase inhibitor and
139 TGF-β receptor inhibitor (**Figure 1A**). Flow cytometry analysis revealed a progressive
140 loss of expression of the epithelial marker, EpCAM, present on iPSCs and upregulation
141 of the mesodermal marker CD56 (NCAM) during the differentiation protocol (**Figure**
142 **1B**).[24] A $KDR^+/PDGFR\alpha^+$ population emerges and peaks at day 4 consistent with the
143 generation of a cardiac progenitor population.[25,26] KDR expression subsequently
144 decreases on day 5 and 6 suggesting advancing maturation of these cardiac progenitors.
145 CCPs are identified as the $CD56^+/PDGFR\alpha^+$ or $CD56^+/CXCR4^-$ population present on day
146 6. Average flow cytometry time course data from 20 runs demonstrate the reproducibility
147 of the differentiation protocol (**Figure 1B, Supplemental Tables 1-4)**. Analysis of gene
148 expression by quantitative RT-PCR over the 6-day protocol revealed loss of expression
149 pluripotency genes (*NANOG, SOX2, POU5F1)* and an increase in expression of cardiac
150 progenitor genes (*HAND2, GATA4, NKX2-5, PDGFRA, TBX5*) (**Figure 1C**). At day 6, the
151 aggregates are dissociated, cryopreserved and described as CCPs.

152 Single cell RNA-sequencing (scRNA-seq) was also performed to better characterize the
153 CCPs. Cryopreserved CCPs were recovered, and a total of 37,014 cells were analyzed
154 using the 10X Genomics Next GEM single cell 3' assay. Chromium single cell data output
155 from the 10X Genomics analysis pipeline were further analyzed using Seurat and
156 Cellxgene VIP software. Transcriptomic analyses of the CCPs identified 7 clusters, and
157 5 clusters were closely related (C0, C1, C2, C4, C6) (**Figure 2A)**. Analysis of differentially

158 expressed genes (DEGs) revealed cardiomyocyte-fated cells in clusters C0, C2, C4 and
159 C6 with expression of genes encoding cardiac transcription factors (*MEF2C, TBX5,*
160 *NKX2-5*), myofilaments (*ACTC1, MYL4, MYL7, MYH6*), EC coupling proteins (*RYR2*) and
161 ion channels (*CACNA1D, KCNIP4, SLC8A1*). These 4 cell populations account for 64%
162 of the total cells in the CCPs and were annotated cardiomyocyte progenitor (CMP)
163 (**Figure 2B,F**). Further analysis of the DEGs and the GO terms showed the C2 and C4
164 cell populations differentially express cell cycle marker genes *MKI67* and *TOP2A*. In
165 addition, C2 cells differentially express *CCNB1* (Cyclin B1) and *CENPA* in contrast to C4
166 cells which express *CDC6* and *FEN1* that are essential for DNA replication, indicating
167 capture of M phase and S phase proliferating CMPs, respectively (**Figure 2E,F,**
168 **Supplement 2**). The small cluster C6 has abundant expression of *TTN* and *RYR2*,
169 suggesting a differentiating cardiomyocyte (CM). Interestingly, cluster C1 that accounts
170 for 15% of the total CCPs has elevated expression of ribosomal genes including *RPLP1*,
171 *RPS15* as well as genes for ATP synthase complex (*ATP5F1E*) and NADH
172 dehydrogenase (*NDUFS5*) in mitochondrial that are essential for protein translation and
173 metabolism along with lower expression of myofilament, EC coupling and ion channels
174 genes than the CMP populations, so we annotated this cell population as a cardiac
175 progenitor (CP) (**Figure 2A,F**). The C3 and C5 clusters account for 12% and 8.6% of the
176 total CCPs, respectively, and have distinct gene expression pattern from the CMP. The
177 C3 cells differentially express typical endodermal marker genes of EPCAM and FOXA2,
178 and C5 cells differentially express typical endothelial marker genes of CD34, CDH5
179 (CD144), and PECAM1 (CD31) (**Figure 2C,D,F)**. Overall, the scRNA-seq analysis
180 confirmed that the CCP preparation is composed primarily of cells fated to become CMs
181 (~80%) whereas a smaller populations of endothelial and endodermal cells are present.

182 *In vitro* potency of CCPs

183 To test the potency of the cryopreserved CCPs, cells were thawed and plated on
184 vitronectin substrate in RPMI+B27 medium and characterized after 7 days of culture. After
185 7 days in culture in RPMI+B27, the cells differentiated into contracting sheets of iPSC-
186 derived cardiomyocytes (iPSC-CMs) (Video supplement 1). Flow cytometry
187 demonstrated that upon thawing 9.3±4.0% of the cells expressed low levels of sarcomeric
188 α-actinin (SAA), but after 7 days of culture 95.9±0.8% of the differentiated cells expressed
189 SAA consistent with differentiation primarily to iPSC-CMs (**Figure 3A**). Immunolabeling
190 of the differentiated cells confirmed that nearly all cells were iPSC-CMs which expressed
191 Nxk2.5, SAA, cardiac troponin I (cTnI), and cardiac troponin T (cTnT) (**Figure 3B**). Optical
192 mapping of the contracting monolayers of iPSC-CMs loaded with a voltage-sensitive
193 fluorescent dye, FluoVolt™, demonstrated optical action potentials with an average
194 spontaneous rate of 1.16±0.02 Hz (n=4). Point stimulation of the cultures over a range of
195 frequencies (1.5-3.0 Hz) showed electrical coupling between the iPSC-CMs with uniform
196 conduction through the monolayers and conduction velocities (CV) ranging from 9.2±0.2
197 to 13.4±0.4 cm/s (**Figure 3C,D)**. The optical action potential durations progressively
198 shortened at higher rates of stimulation consistent with rate adaptation of cardiac action
199 potentials (**Figure 3C,D).** Single iPSC-CMs (n=27) were characterized with perforated
200 patch clamp recording and demonstrated action potentials when stimulated at 1 Hz with
201 an average maximum diastolic potential (MDP) of -72.5±1.1 mV, action potential
202 amplitude (APA) of 107.0±1.7 mV and dV/dt_{max} of 112.1±14.5 V/s **(Figure 3E,**
203 **Supplemental Table 5)**. These results show that thawed CCPs plated in basal
204 RPMI+B27 medium without additional growth factors or small molecules rapidly

205 differentiate predominantly to iPSC-CMs and exhibit electrophysiological properties
206 typical of early developing human cardiomyocytes.

207 To determine the potency of CCPs to differentiate into iPSC-derived endothelial cells
208 (iPSC-ECs), thawed CCPs were plated in an endothelial medium, Vasculife LS1020™.
209 After 12 days in culture, flow cytometry demonstrated that 88.0±1.3% of cells were
210 $CD31^+/CD144^+$ iPSC-ECs (**Figure 3F**). Further characterization of the $CD31^+/CD144^+$
211 population shows that 15.2±1.2% of the cells express CXCR4, a marker of arterial
212 endothelial cells (**Figure S1)**.[27,28] Immunolabeling of the day 12 cultures also
213 demonstrated expression of CD31 in a monolayer of human iPSC-ECs (**Figure 3F)**. To
214 test the functional properties of the iPSC-ECs, a matrigel tube formation assay was
215 carried out on replated day 12 cells. One day after replating, the iPSC-ECs organized into
216 an interconnected network of tubes in Matrigel (**Figure 3G)**. Thus, in medium optimized
217 for EC culture, CCPs readily differentiate to iPSC-ECs.

218 <u>CCPs engraft in swine infarcted myocardium and differentiate to cardiac lineages</u>

219 A total of 70 pigs underwent LAD balloon occlusion reperfusion, of which 52 survived the
220 post-MI period to treatment (**Figure S2**). Of the remaining 52 pigs, 6 pigs were evaluated
221 in the roll-in feasibility cohort which underwent open-chest epicardial injections of
222 CCPs+cECM after 4 weeks post-MI. Pigs were sacrificed 2 weeks later, and hearts were
223 sectioned for histopathology. The other 46 pigs were randomly assigned to one of four
224 treatment groups: CCP+cECM, CCP alone, cECM alone or Control (5% Flexbumin).
225 Entry of pigs into the cECM alone cohort was stopped after only 3 pigs were treated due
226 to lack of a clear trend toward improved ejection fraction and limitations on animal

227 numbers. Thus, the functional studies focused on comparing 3 groups: CCPs,
228 CCPs+cECM, and control.

229 In the feasibility roll-in cohort, pigs were followed for 2 weeks post cell delivery, and the
230 presence of engrafted human cells was assessed by immunolabeling for human nuclear
231 antigen, Ku80, or human mitochondria. All 6 pigs demonstrated Ku80 positive human cell
232 grafts that were composed largely of cTnI co-labeled cells; however, cTnI labeling
233 intensity was less than observed in the native pig myocardium (**Figure 4A**). Trichrome
234 staining of an adjacent section revealed the corresponding human cell grafts adjacent to
235 the native myocardium (**Figure 4B**). Human cell grafts were identified within the scar and
236 in adjacent native myocardium (**Figure 4C-E**). The grafts were composed predominantly
237 of human cardiomyocytes based on the cTnI immunolabeling, but the sarcomeric pattern
238 and density of labeling was consistent with immature cardiomyocytes. In addition, using
239 co-labeling with an antibody detecting human mitochondria and an antibody for CD31, we
240 detected human endothelial cells in the grafts (**Figure 4F-I**). These results demonstrate
241 that the CCPs can survive following injection into the post-MI porcine heart and
242 differentiate into cardiomyocytes and endothelial cells to form cardiac tissue grafts.

243 In the randomized phase, pigs were sacrificed at 4 weeks post-treatment, although a
244 small subset of pigs were survived up to 8 weeks after transendocardial delivery
245 (**Supplemental Table 6** for summary of randomized pigs and analysis). In pigs receiving
246 CCPs with or without cECM, hearts were systematically blocked, and sections were
247 immunolabeled for human Ku80 and cTnI. Human grafts were identified in 13/14 (92.9%)
248 of pigs in each the CCPs and CCPs+cECM cohorts. The graft area observed on the
249 histological sections were comparable between the CCP and CCP+cECM groups (0.68
250 +/- 0.25 mm^2 and 0.37 +/- 0.168 mm^2, respectively, p=0.30, supplemental **Figure S4D**).

251 Furthermore, the number of graft areas detected was comparable between the CCP and
252 CCP+cECM groups (5.8±2.2 and 5.2±1.6, p=0.57, **Supplemental Figure S4E**)
253 Macroscopic graft size was not measured given the blocking strategy used to enable
254 detailed histological characterization of the large porcine hearts. In the animals sacrificed
255 4 weeks after CCP delivery, we quantitatively analyzed the cellular composition of the
256 grafts by co-labeling for lineage specific markers and Ku80. The vast majority of $Ku80^+$
257 cells co-labeled with cTnI (~90%, **Figure 5A,D**) indicating cardiomyocytes. Less than 1%
258 of the $Ku80^+$ cells were endothelial cells based on CD31 labeling (**Figure 5B,D)** and 1-
259 2% of the $Ku80^+$ cells were vimentin positive stromal cells (**Figure 5C,D)**. Both CCP and
260 CCP+cECM groups showed similar cellular compositions of the grafts. A small fraction
261 (<10%) of the cellular composition of grafts could be other cell types not evaluated for
262 including possible residual CCPs, which were not assessed given the lack of a unique
263 marker to distinguish them from native myocardium. There were no areas of
264 osteochondral differentiation.[29] Grafts were present in both CCP and CCP+cECM animals
265 up to the latest time point sampled, 8 weeks after delivery.

266 <u>CCP-derived grafts show progressive maturation of ventricular cardiomyocytes</u>

267 To assess the chamber-specificity of the differentiated cardiomyocytes in the grafts and
268 to examine for evidence of maturation, we immunolabeled sections with an antibody
269 recognizing the ventricular-specific myosin light chain, MLC2v at 2-, 4- and 8-weeks post-
270 transplant. Most of the human cells identified using an anti-human mitochondrial antibody
271 expressed MLC2V at all time points tested (**Figure 5G-L, Figure S5)**. There was
272 evidence of progressive sarcomere organization and maturation based on the pattern of
273 MLC2v labeling from 2 weeks to 8 weeks, although the cells remained smaller and with
274 less sarcomere organization than adjacent adult porcine myocardium. Together these

275 results demonstrate that transendocardial delivery of CCPs in the post-MI swine heart
276 leads to formation of cardiac grafts predominantly composed of human ventricular
277 cardiomyocytes with occasional human endothelial cells and stromal cells. The grafts
278 persist for the 8 weeks of observation in this immunosuppressed swine model and show
279 evidence of progressive cardiomyocyte maturation.

280 Cardiac MRI assessment

281 Twenty-two pigs were evaluable for MRI in the three experimental groups, whereas 19
282 pigs were excluded from the MRI analysis due to: LVEF >45% (n=1), infarct size <8% of
283 LV (n=1), hemodynamically significant opportunistic sepsis/infection (n=13), and
284 technical issues with the MRI acquisition (n=4) (see **Supplemental Figure 1,**
285 **Supplemental Table 6**). Prior to CCP delivery, there was no significant difference in
286 baseline post-MI left ventricular ejection fraction: CCPs alone (n=5) 43.8 +/- 4.3%, and
287 CCPs+cECM (n=9) 39.9 +/- 4.1%, and Control (n=8) 44.8 +/- 4.2%. Four weeks following
288 transendocardial delivery, no statistically significant change in ejection fraction was
289 observed for any of the three groups, but CCPs trended to improvement (p=0.08), while
290 CCPs+cECM (p=0.3) and control injections (p=0.99) showed no clear improvement
291 (**Figure 6A,B)**. Similarly, there was no statistically significant difference between groups
292 in left ventricular end-diastolic volume and left ventricular end-systolic volume following
293 intramyocardial injection (**Figure 6C,D)**. Late gadolinium enhancement-determined
294 infarct volume was not significantly changed in any of the three groups (**Figure 6E,F)**.

295 Pressure-volume hemodynamic analysis shows CCPs improve EF and contractility
296 reserve

297 Invasive hemodynamic pressure-volume (PV) studies were performed at the endpoint of
298 the study for each animal (**Figure 7A-C)**. Only pigs meeting the MRI inclusion criteria
299 above (EF<45% or infarct >8% of LV, free of infection) and sacrificed at the 4-week
300 timepoint were considered potentially evaluable by PV loop analysis. Technical problems
301 during PV-loop acquisition or poor-quality loops caused the exclusion of 3 additional
302 animals. Comparison of resting ejection fractions from the hemodynamic studies
303 demonstrated a significantly higher ejection fraction in the CCP (46.1 ±1.8%) group
304 compared to Control (37.1 ±2.0%) (p=0.007), and the CCP+cECM (43.3 ±1.3%) group
305 showed a trend to improvement (**Figure 7D**). End systolic volume was significantly
306 reduced in CCP (49.1 +/-3.0 ml) and CCP+cECM (51.3 +/-1.7 ml) groups compared to
307 Control (75.3 +/-5.6 mL) (p=0.0004 ANOVA; p=0.001 and p<0.0001 respectively) (**Figure**
308 **7E**). End diastolic volume was also significantly reduced in CCP (91.0 +/-5.1 ml) and
309 CCP+cECM (90.5 +/-2.9 ml) groups compared to the Control group (119.3 +/-6.0 ml)
310 (p=0.0006 ANOVA; p=0.003 and p=0.001 respectively) (**Figure 7F)**. There was no
311 significant difference in end systolic elastance between CCP, CCP+cECM and Control
312 groups at baseline (p=0.13 ANOVA). Following dobutamine challenge to assess
313 contractile reserve, a significant increase in elastance was observed in all groups (CCP
314 alone (8.4 +/-0.9) and CCPs+cECM (4.5 +/-0.7) control (4.4 +/-0.7) (compared to baseline
315 (p=0.0002, p=0.004, and 0.04 respectively) (**Figure 7G)**. The CCP alone group showed
316 significantly greater elastance in the presence of dobutamine relative to Control (p<0.006)
317 and CCP+cECM (p=0.007).

318 <u>Safety evaluation shows no CCP-induced ventricular tachycardia</u>

319 Safety assessment for the study included evaluation of procedure related complications,
320 gross or histological tumor formation, and arrhythmias. In all treated pigs, there were no

321 procedure related adverse events such as cardiac perforation, MI, stroke, or limb
322 ischemia. Continuous electrocardiographic monitoring for significant tachycardia (>150
323 bpm for greater than 24 beats) using an implanted cardiac monitor (REVEAL LINQ™)
324 was performed from the time of the initial MI until pigs were sacrificed, in both the initial
325 feasibility cohort and the randomized cohort. There was only one episode of sustained
326 ventricular tachycardia (>30 seconds) that self-terminated in one randomized cohort pig
327 treated with CCP+cECM on post-injection day 2 (**Figure 8B**). This animal (4680) also
328 exhibited post-MI ventricular tachycardia prior to cell delivery. There was one brief run of
329 ventricular tachycardia (10 s) detected in a CCP treated pig on post-injection day 11
330 (**Figure 8 A,E**). Otherwise, there were no episodes of ventricular tachycardia or
331 ventricular fibrillation detected in any of the pigs treated with CCPs followed for up to 8
332 weeks. Immunolabeling for the gap junction protein, connexin 43 (Cx43), did show
333 relatively sparse expression of Cx43 within the graft relative to native myocardium and
334 occasionally between graft cardiomyocytes and native myocardium (**Figure 8F)**. Finally,
335 necropsy did not reveal evidence of gross tumors in any animal, and there was no cardiac
336 histological evidence of tumor formation observed.

337

338 **DISCUSSION**

339 In this preclinical study, we tested the ability of minimally invasive TEI delivery of a novel
340 human iPSC cell product, CCPs, alongside a retention biomaterial to remuscularize the
341 porcine post-MI myocardium. The major findings are: i) transplanted CCPs differentiate
342 to form grafts composed primarily of cTnI and MLC2v positive ventricular cardiomyocyte
343 and occasional human CD31 positive endothelial cells, ii) neither transplant of CCPs or
344 CCPs+cECM significantly improved cardiac MRI measured ejection fraction or cardiac

volumes, but the CCP and CCP+cECM groups demonstrated significantly greater contractile reserve relative to control by invasive hemodynamic assessment, iii) CCP +/- cECM administration was feasible without adverse safety outcomes including no tumor formation and no ventricular arrhythmias, and iv) human iPSC-CMs in grafts displayed progressive maturation but remained structurally immature at 8 weeks post injection. Together, these results demonstrate that CCPs hold promise as a therapy for the post-MI heart.

The concept of using cardiac progenitor cells for post-MI heart failure treatment has been investigated in a variety of contexts. The adult heart does not contain a pool of stem or progenitor cells with potency to generate new heart muscle,[30,31] but hPSCs provide an accessible and clinically relevant source of cardiac progenitor cells. However, hPSC-derived cardiac progenitor cell populations are heterogenous and dynamic during differentiation akin to cardiac development in which different progenitor populations gradually give rise to distinct heart regions and structures. An early study using *in vitro* engineered heart tissue comparing mouse ESC-CMs and ESC-derived Flk1$^+$/PDGFRα$^+$ cardiac progenitor cells demonstrated that the cardiac progenitor cells differentiated to CMs and improved the electrical coupling in the engineered heart tissue more effectively than the ESC-CMs.[32] Using similar cell preparations from hESCs, a study comparing hESC-CMs to KDR$^+$/PDGFRα$^+$ cardiovascular progenitor post-MI in a nude rat model showed comparable grafts and functional effects from the two populations.[33] A developmentally earlier mesodermal SSEA1$^+$ cell population derived from rhesus ESCs was shown to engraft and differentiate to cardiomyocytes, populating 20% of the scar region in the post-MI rhesus heart.[34] However, a more recent study of the xenogeneic transplantation of hESC-derived SSEA1$^+$ cells post-MI nonhuman primate hearts found

369 no human cells remaining at 140 days, although an improvement in cardiac function was
370 observed and attributed to decreased apoptosis of endogenous cardiomyocytes.[35]
371 Likewise, transplantation of hESC-derived SSEA1^{+} cells in fibrin patches in a rat MI model
372 showed improvement in LV function despite lack of survival of the transplanted cells,
373 suggesting a paracrine mechanism of action.[36] Studies using an intermediate stage
374 cardiac progenitor population first identified by high levels of Isl1 expression showed in
375 rhesus heart slice models that the cardiac progenitors are highly migratory and can track
376 to areas of cryoinjury.[37] In post-MI porcine model, the same cardiac progenitors engrafted
377 and formed cardiomyocyte rich grafts, but there was no statistically significant
378 improvement in MRI measures of LV function after 12 weeks.[37] Yap et al.,[19] provided
379 evidence that late-stage or committed cardiac progenitors can be effectively delivered at
380 the time of surgically induced MI, engraft and differentiate to relevant cardiac lineages
381 forming cardiomyocytes rich grafts lasting at least 2 months with evidence for
382 improvement in EF from cardiac MRI.[19] However, the study by Yap et al., found evidence
383 for ventricular arrhythmias following cell delivery in approximately half of the treated
384 animals.[19] In the present study, we used late stage CCPs, but unlike prior studies they
385 were differentiated from hiPSCs rather than hESCs. Furthermore, although scRNA-seq
386 analysis showed heterogeneity in our CCP preparation, more than 80% of the cells were
387 cardiomyocyte-fated in contrast to the Yap et al. which identified 33% of the cells as
388 cardiac progenitors.[19] The present study used clinically relevant TEI delivery one month
389 following infarct in contrast to prior studies using surgical, epicardial injection in the acute
390 or subacute phase of MI. Comparable to earlier studies, we observed engraftment and
391 differentiation to form cardiac muscle grafts, but there was not an improvement in cardiac
392 function on cardiac MRI evaluation despite an improvement in dobutamine recruitable

393 functional reserve. The mechanism underlying the improvement in functional reserve
394 could reflect a less advanced stage of heart failure in which β-adrenergic signaling is less
395 desensitized which may be due to a paracrine mechanism or a direct contribution of
396 engrafted cells unmasked by β-adrenergic stimulation. In summary, studies using hPSC-
397 derived cardiac progenitor cells in animal models post-MI demonstrate the ability of the
398 cells to engraft and differentiate with variable evidence for improvement in cardiac
399 function and risk of ventricular arrhythmias.

400 Significant safety concerns due to ventricular arrhythmias following delivery of hPSC-CMs
401 by epicardial injection in large animal post-MI heart failure models have arisen, although
402 the arrhythmias are generally transient, starting within 1 week after transplant and lasting
403 approximately one month.[11,15,17] Current evidence suggests that these ventricular
404 arrhythmias are the result of rapid intrinsic automaticity arising from a subpopulation of
405 engrafted CMs rather than reentry mechanisms.[13,16] The sustained ventricular
406 tachycardia has been tolerated in nonhuman primate models following cell therapy, but
407 in porcine models, there has been significant mortality observed in treated animals.[11,38]
408 Pharmacological treatment with ivabradine and amiodarone reduced the engraftment
409 arrhythmia burden but did not eliminate it.[38] Given that abnormal automaticity is the
410 presumed basis for these ventricular arrhythmias, gene editing was used to alter
411 expression of 4 different ion channels and transporters to eliminate automaticity.[14] This
412 approach greatly reduced engraftment arrhythmias, although there was still an early
413 period of sustained ventricular tachycardia. The arrhythmic risk for cardiac progenitor
414 cells is less clear as some of the large animal studies did not directly monitor for
415 arrhythmias.[34] However, Yap et al. observed that approximately half of the treated pigs
416 with CCPs developed sustained ventricular tachycardia starting 9 days or later and lasting

417 at least a month and in one animal up to week 12, which appears slightly delayed relative
418 to the hPSC-CM studies. This potentially reflects the additional time needed for
419 differentiation of CCPs. In contrast, the present study observed one relatively short
420 episode of nonsustained ventricular tachycardia in all of the CCP and CCP+cECM treated
421 animals which was in an animal exhibiting runs of ventricular tachycardia prior to cell
422 therapy. The mechanisms underlying the minimal arrhythmic burden in the present CCP
423 study will require further investigation, and potential considerations include differences in
424 the cell population, TEI vs. epicardial delivery, graft size or localization, and time after MI
425 for therapy. Our working model is that gradually differentiating CMs from the CCPs
426 integrate into the native myocardium in smaller, distributed endocardial grafts entrained
427 by the surrounding myocardium without coalescing into large grafts. Future mechanistic
428 studies of electrical integration of the predominantly endocardial cellular grafts resulting
429 from TEI will require alternative approaches from previously successful surface optical
430 mapping of whole heart epicardial grafts.[16] Furthermore, differences in arrhythmia
431 surveillance approaches may contribute to some differences in observed arrhythmia
432 burden between studies as investigations using implanted loop recorders such as this
433 one, rather than continuous telemetry, will not detect slower ventricular tachycardia (<150
434 bpm in this study). Ultimately identifying the key factors that eliminate or minimize the
435 arrhythmia risk is necessary for this therapy to advance successfully to the clinic.

436 Combining cell products with matrix preparations or synthetic hydrogels has been
437 demonstrated in previous studies to improve cell retention and survival in post-MI hearts.
438 For example, the pro-survival cocktail used in several studies includes the complex matrix
439 preparation, Matrigel™.[5] Gelatin hydrogels have been used successfully in the
440 transplantation of iPSC-CM cardiomyocytes spheroids in post-MI animal models.[39] In this

441 study, we tested the addition of an injectable formulation of cECM to the CCP product,
442 but this did not result in improved functional benefits at the cECM dose delivered;
443 however, we did find an increase in the number of epicardial grafts on the surface of the
444 heart in the cECM+CCP group relative to CCP alone. This may be related to cECM
445 helping retain any cells that get into pericardial space. How this potential differential
446 localization of grafts impacts long-term outcomes will require additional study. In addition,
447 cECM has been proposed to have favorable immunomodulatory effects via alternatively
448 activated macrophage education,[21] which could theoretically make local, ischemic tissue
449 more hospitable for co-transplanted cells. However, these favorable influences may be
450 blunted in this immunosuppressed animal model. Overall, the tested delivery of cECM did
451 not improve functional outcomes in this study, but additional studies are needed to
452 determine the optimally formulated and dosed delivery vehicle to promote cell survival
453 and engraftment.

454 TEI delivery has emerged as an appealing, minimally invasive approach for direct
455 intramyocardial transplantation of cells, biomaterials and other biologic agents in a
456 targeted fashion. In a recent pooled analysis, this delivery approach was observed to be
457 overall safe in >1800 patients injected in clinical trials worldwide[40]. In this study, the
458 NOGA/Myostar (Biosense Webster/J&J) mapping and TEI catheter platform was used to
459 perform targeted injections; however, this platform was recently discontinued from
460 production by the manufacturer. Alternative cardiac mapping approaches to facilitate
461 accurate targeting with TEI, such as co-registered multimodality imaging, have been
462 described but remain investigational.[41] Similarly, alternative investigational TEI catheters,
463 such as the helical needle-tipped “Helix” catheter (BioCardia, Sunnyvale, CA), are being
464 actively used in active adult cell therapy trials[42,43]. These novel cardiac visualization

465 methods and catheter designs may pave the way to help inject a new generation of
466 therapeutic cells designed to remuscularize the damaged heart.

467 Overall, the optimal hPSC cell product and delivery strategy to remuscularize the heart
468 remains to be determined. Even a combination of cell products may be preferable such
469 as hiPSC-derived endothelial cells and hiPSC-CMs to promote cell survival and
470 revascularization.[44] Ground breaking phase 1 clinical trials are testing hPSC-CMs to treat
471 heart failure employing epicardial injections,[45] transcatheter injections (NCT04982081)
472 and epicardial patches (NCT04945018, NCT04396899) are underway world-wide as well
473 as a completed trial demonstrating the safety of hESC-SSEA1^{+} progenitor cells
474 transplanted at the time of coronary artery bypass grafting surgery.[18] Despite these
475 developments, important unanswered questions remain including concerns about
476 immunogenicity, repeat dosing possibilities, electromechanical integration,
477 arrhythmogenicity, and whether minimally invasive transcatheter administration will be
478 feasible for wider adoption of this therapy.

479 Nevertheless, early phase clinical trials are underway testing the safety of delivering
480 hPSC-CMs in patients with heart failure with reduced ejection fraction either by direct
481 intramuscular injection or transplantation of cellularized sheets to the epicardium
482 [clinicaltrials.gov NCT03763136; NCT04945018; NCT03763136; NCT04696328;
483 NCT04945018].

484 Limitations

485 Following cardiac transplantation of the CCPs, we identified the progeny of the CCPs to
486 predominantly include cardiomyocytes and more rare endothelial cells and fibroblasts;
487 however, we cannot exclude other small populations of cell types including residual

488 CCPs. We did not observe tumor formation which suggests that the cell preparation did
489 not include pluripotent stem cells capable of forming teratomas. The dosing of CCPs was
490 based on the literature and pilot studies of epicardial injected CCPs, so improvements in
491 dosing and repeat dosing could positively impact outcomes. The current study did not
492 provide long-term follow-up of the animals, in part due to the challenge of opportunistic
493 infections in the setting aggressive immunosuppression. There was qualitative evidence
494 of maturation over 2 months based on myofilament organization, but no quantitative
495 measure of maturation was made. Infections also caused a reduction in the planned
496 sample size. Electrical integration of the cells was not directly examined in this study, but
497 it will be an important subject of future research to define the mechanisms leading to lack
498 of arrhythmias in our study relative to hPSC-CMs studies.

499

500 **Acknowledgements:**

501 Sincere thank you to Allison Rodgers, Everett Temme, Sarah El Meanawy and Vivian
502 Hacker for animal handling and procedures, and Emily Ferris for MRI acquisition and
503 analyses.

504 **Sources of Funding**

505 Funding support provided by:

506 1. National Institutes of Health 5U01HL148690-02
507 2. National Institutes of Health T32 HL007936
508 3. Fujifilm Cellular Dynamics, Inc, Madison, WI
509 4. Cellular Logistics, Inc., Madison, WI
510 5. University of Wisconsin-Madison

511 **Disclosures**

512 ANR: Research or educational grants from Fujifilm Cellular Dynamics, Siemens
513 Healthcare, BioCardia. Consultant for Blue Rock Therapeutics and Novo Nordisk. Co-
514 founder with equity interest in Cellular Logistics, Inc.

515 EGS: Co-founder with equity interest in Cellular Logistics, Inc.

516 CK, MB, KS, and EH are employees of Fujifilm Cellular Dynamics, Inc.

517

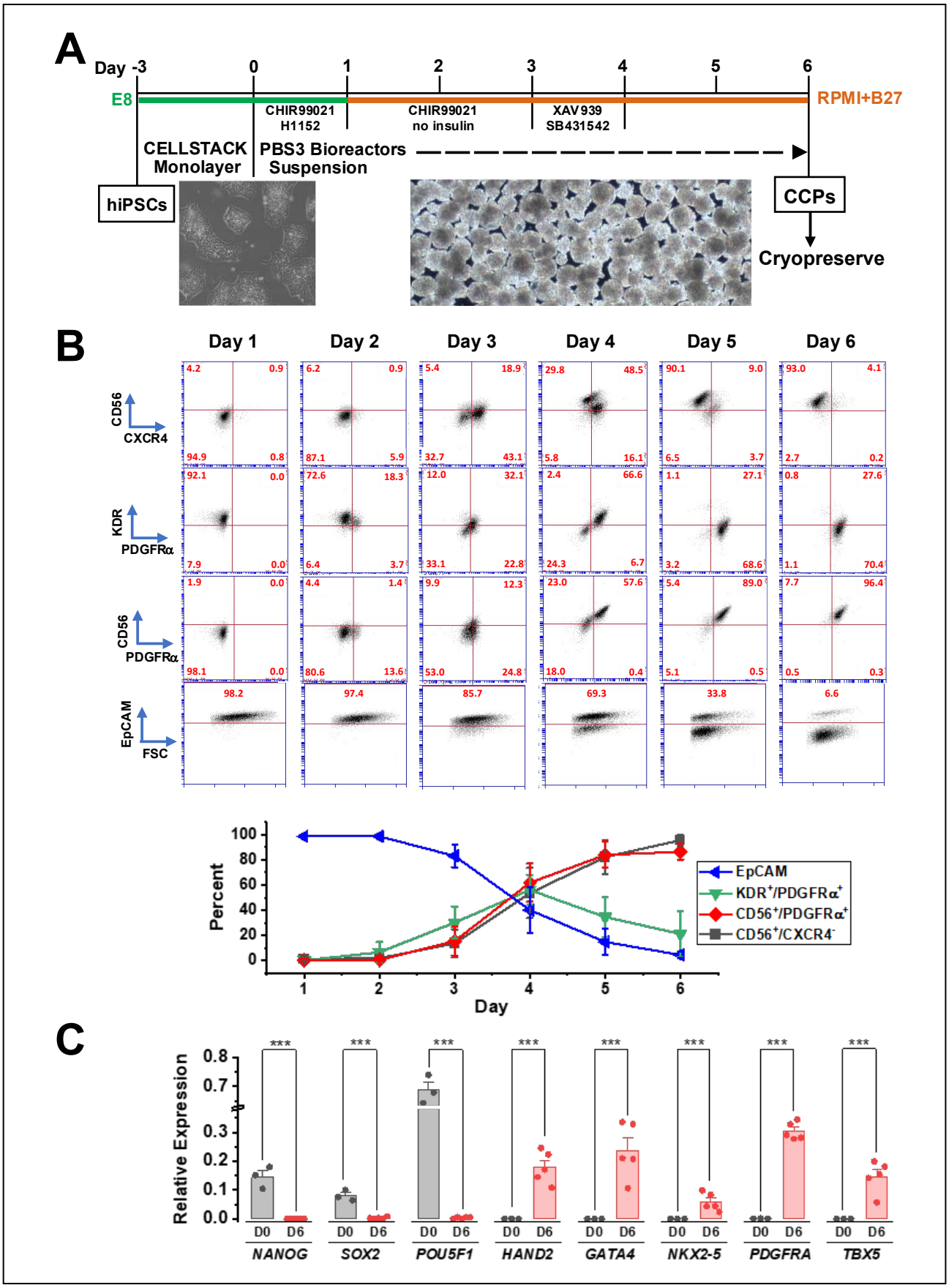

518 **Figure 1. Differentiation of human iPSCs to CCPs. A)** Differentiation schematic to

519 manufacture CCPs with images showing starting aggregates of human iPSCs and final
520 aggregates of CCPs. **B)** Time course of differentation characterizing cell surface protein
521 expression of CD56, KDR, PDGFRα, and EpCAM using flow cytometry from a
522 representative experiment with average data from 7-20 different runs, error bars ±S.D. **C)**
523 Gene expression of pluripotent and cardiac-specific genes at day 0 (iPSCs) and day 6
524 (CCPs) relative to the ribosomal protein *RPL32*. Error bars ±S.E.M., ***$p<0.005$ by t-test
525 comparison.

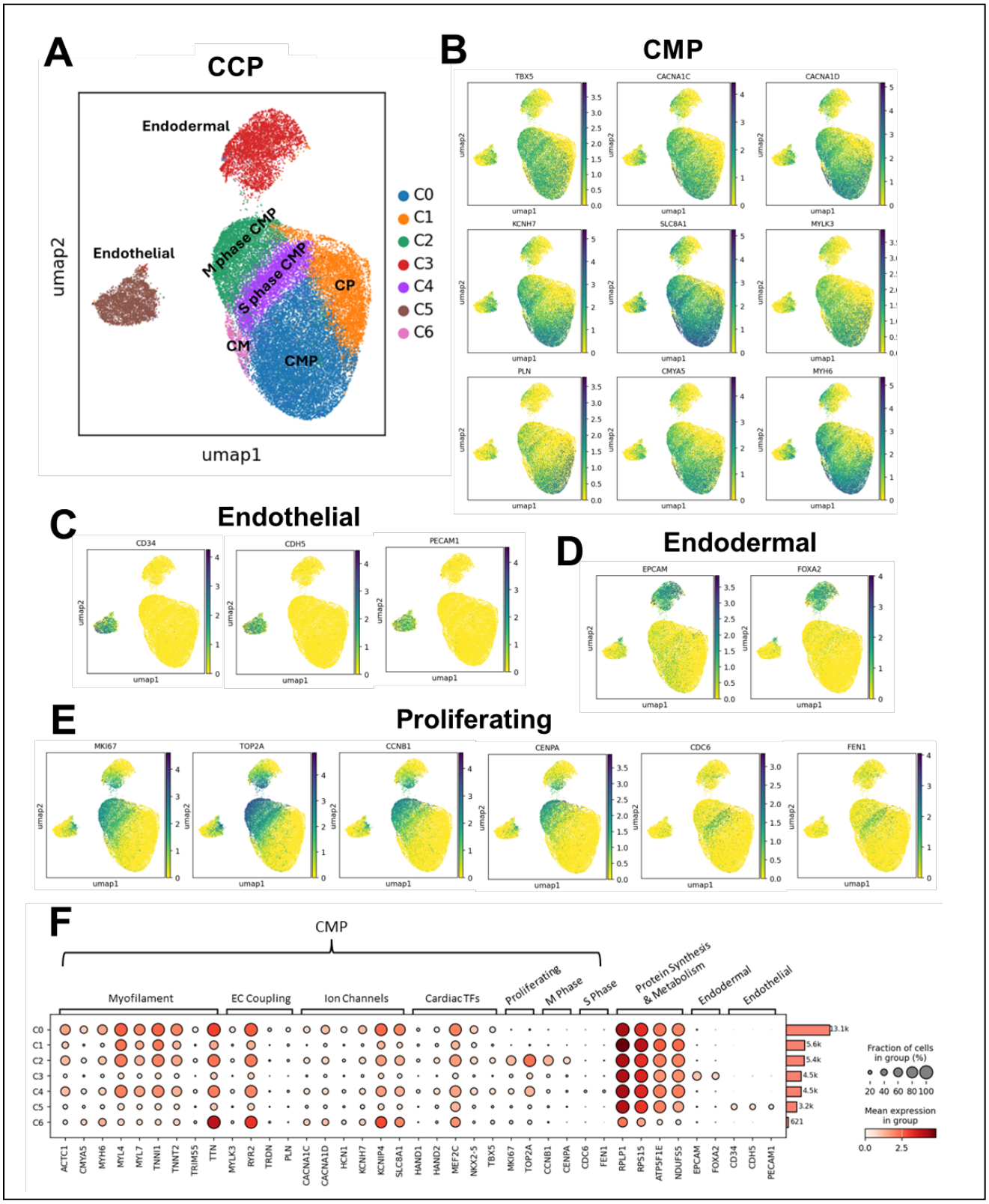

Figure 2. Single cell RNA-sequencing analysis of CCPs. A) UMAP projection for CCPs identifies 7 cell clusters annotated based on differential gene expression. **B-E)** Embedding plots for expression of cardiac marker genes in CMP, endothelial cell, endodermal cell, and proliferating cell, respectively. Scale is log2 fold change. **F)** Dot plot

530 showing expression of representative marker genes used to annotate the clusters. CMP:
531 cardiomyocyte progenitor; CP: cardiac progenitor; CM: cardiomyocyte.

532

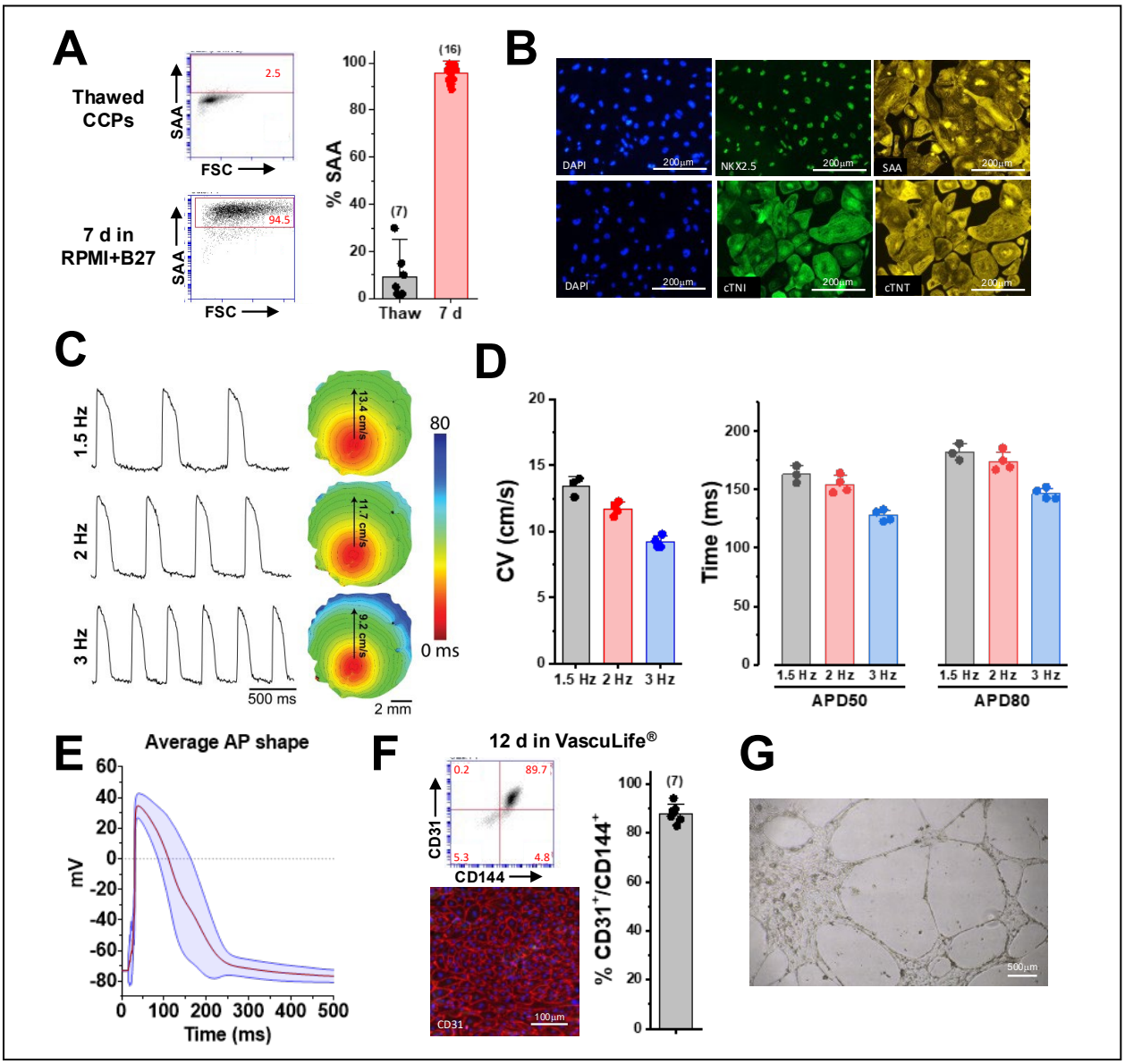

533 **Figure 3. In vitro differentiation of CCPs to iPSC-CMs and iPSC-ECs. A)** Flow
534 cytometry analysis of CCPs immediately after thaw and following 7 d of culture on
535 vitronectin in RPMI+B27 for sarcomeric α-actinin (SAA) expression. **B)** Immunolabeling
536 of differentiated CCPs after 7 d of culture in RPMI+B27 for cardiomyoctye markers
537 Nkx2.5, SAA, cardiac troponin I (cTnI) and cardiac troponin T (cTnT). **C)** Optical action
538 potentials measured at 1.5, 2.0, and 3.0 Hz stimulation from differentiated iPSC-CM
539 monolayers loaded with Fluovolt™ with conduction maps shown to right. **D)** Average data
540 from optical action potentials for conduction velocity (CV) and action potential duration at
541 50% (APD50) and 80% (APD80) of repolarization. **E)** Average perforated patch clamp
542 recorded action potential in red and SD in blue for 27 iPSC-CMs. **F)** Flow cytometry for
543 endothelial markers CD31 and CD144 after 12 days culture of CCPs in Vasculife LS1020

544 medium and immunolabeling (bottom left panel) for CD31. **F)** Dissociated day 12 cells in
545 Vasculife LS1020 plated for one day in undiluted Matrigel form tubes demonstrated by
546 phase contrast micrograph.

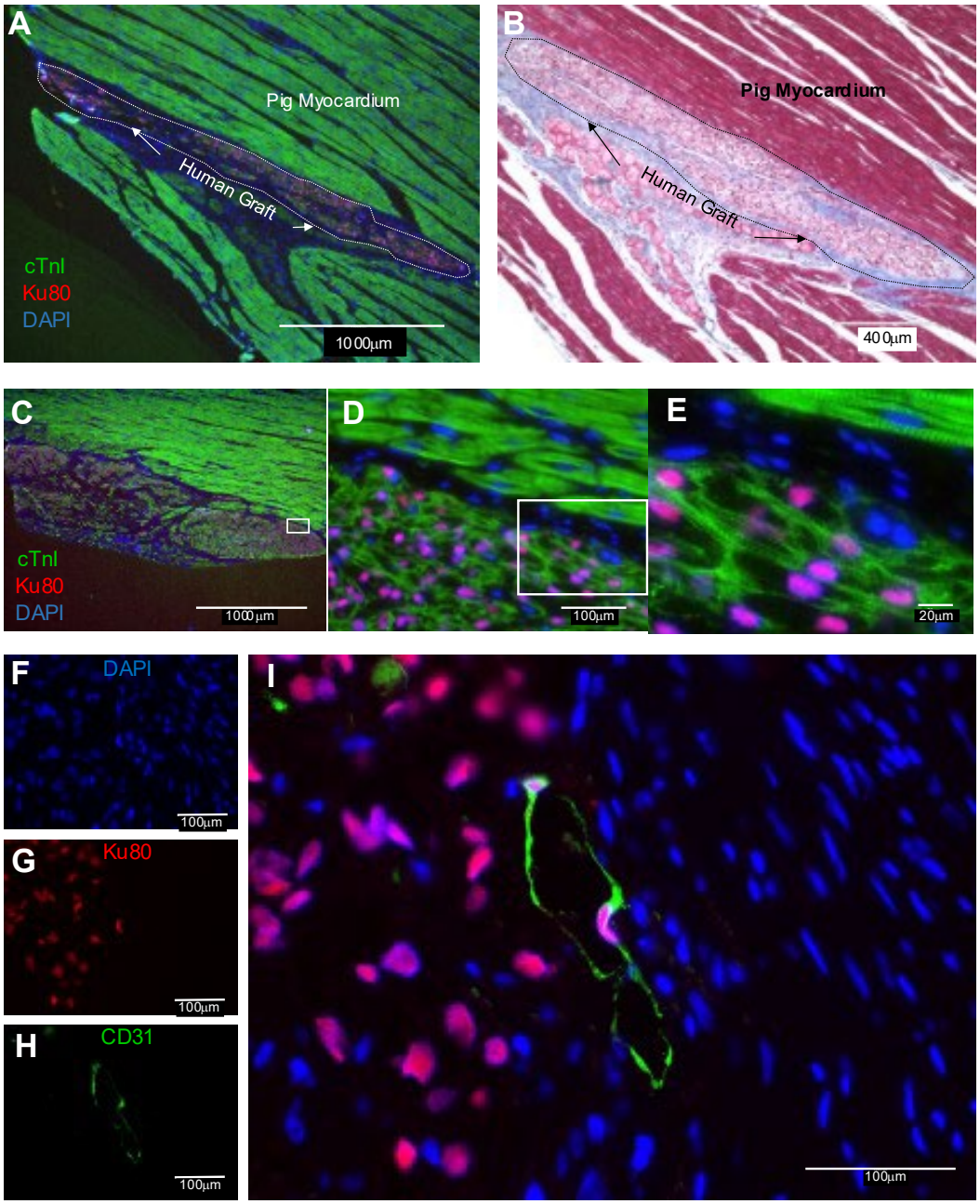

547 **Figure 4. iPSC-CCPs engraft and differentiate to cardiomyocytes and endothelial**
548 **cells 2 weeks after delivery in post-MI swine heart. A)** Epifluorescence image of
549 porcine heart section with human graft identified by Ku80 immunolabeling and
550 cardiomyoctyes by cTnI immunolabeling. **B)** Light microscopic image of adjacent
551 histological section stained with Mason's Trichrome. **C-E)** Immunofluorescence images
552 of human graft in porcine myocardium immunolabeled as indicated identifies human
553 cardiomyocytes. **F-I)** Immunofluorescence image of another human graft in porcine

554 myocardium labeled with anti-Ku80 and anti-CD31 to identify human endothelial cells in
555 the graft.

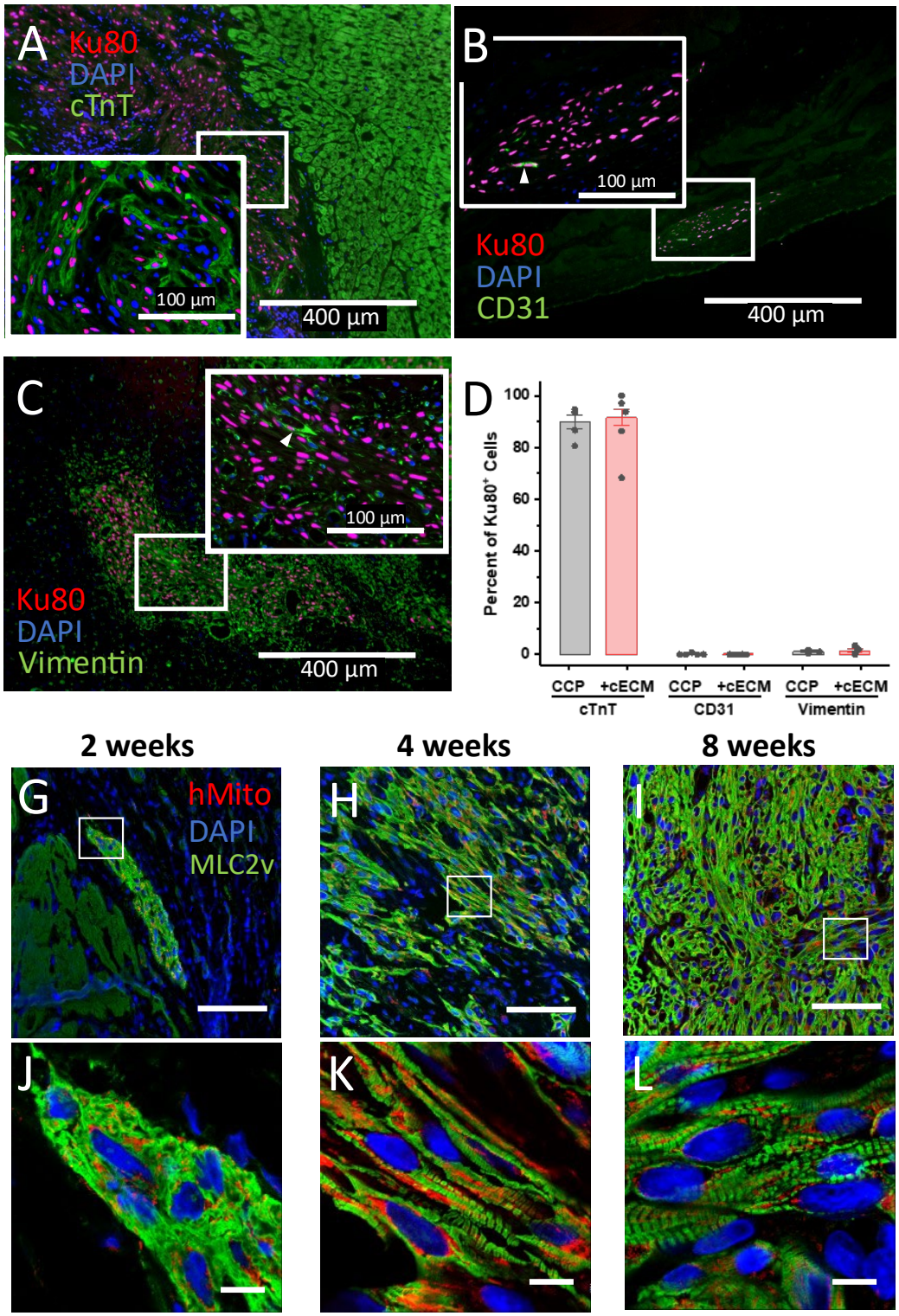

Figure 5. CCP graft composition and maturation. A) Immunofluorescence image of 4-week CCP graft dual immunolabeled for cTnT (cardiomyocytes) and Ku80⁺ to detect human cells with DAPI nuclear labeling. **B)** Immunofluorescence image of 4-week CCP graft dual immunolabeled for human CD31 (endothelial cells) and Ku80⁺ with DAPI

560 indicating nuclei. Arrowhead indicates example of human endothelial cells ($CD31^+$ and
561 $Ku80^+$). **C)** Immunofluorescence image of 4-week CCP graft dual immunolabeled for
562 vimentin (stromal/fibroblasts cells) and $Ku80^+$ to identify human cells. Arrowhead
563 indicates example of human stromal cell ($vimentin^+$ and $Ku80^+$). **D)** Summary data for
564 graft composition of cardiomyocytes (cTnT), endothelial cells (CD31), and
565 stromal/fibroblast (vimentin) per animal (% of total $Ku80^+$ cells) at 4-weeks after CCP or
566 CCP+cECM delivery. Bar is average and error bars are SEM, n=4-9. There are no
567 significant differences between CCPs and CCP+cECM for any of the markers. **G-L)**
568 Confocal immunofluorescence images of CCP-derived grafts at time points indicated
569 post-delivery immunolabeled for ventricular-specific MLC2v and human-specific
570 mitochondrial antibody with DAPI to identify nuclei. There is progressive maturation of the
571 MLC2v myofilament pattern with increased organization and density of myofilaments with
572 time. Upper row scale bar 200 μm, and lower row expanded inset from indicated region
573 in white box with scale bar 10 μm. Individual channels for panels J,K,L are in
574 supplemental Figure S5.

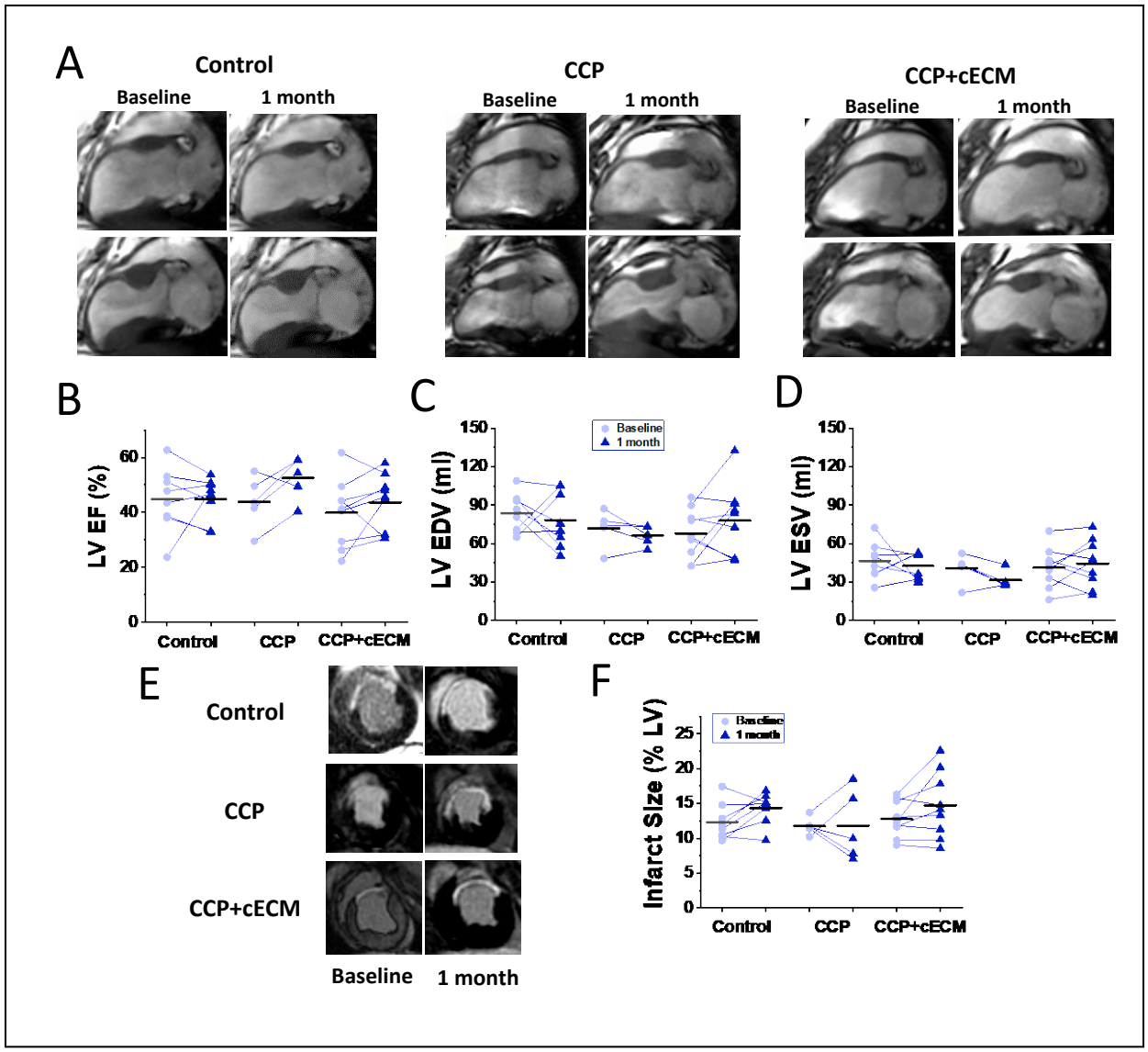

575 **Figure 6. Cardiac MRI analysis. A)** Representative diastolic (upper) and systolic (lower)
576 cardiac cine MR images from Control, CCP only and CCP+cECM treated animals. **B-D)**
577 Comparisons of baseline and 4 weeks after treatment of LVEF, LVEDV and LVESV
578 showed no statistically significant differences between groups. **E)** Representative cardiac
579 MRI viability images. **F)** Comparisons of baseline and 4 weeks MRI infarct size showed
580 no significant differences.

581 CCP = committed cardiac progenitor cells, cECM = cardiac extracellular matrix, LVEF =
582 left ventricular ejection fraction, LVEDV = left ventricular end diastolic volume, LVESV =
583 left ventricular end systolic volume.

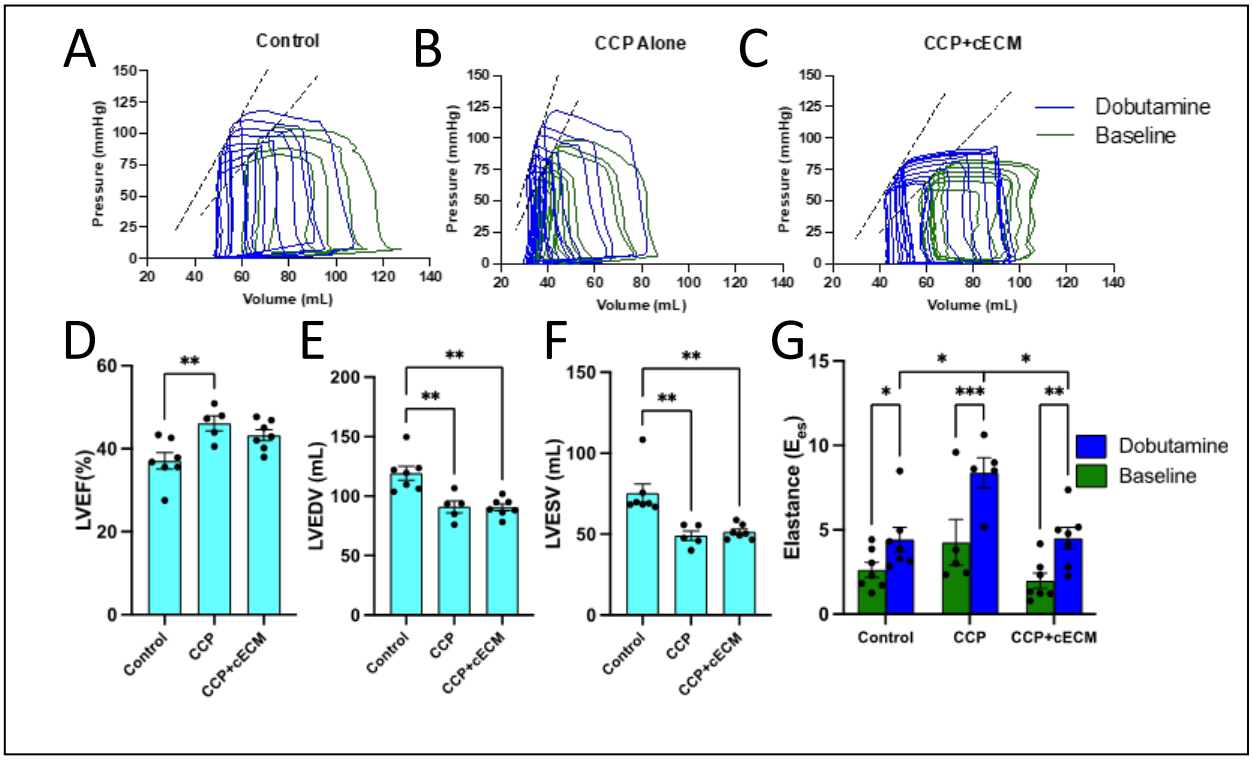

584 **Figure 7. Invasive hemodynamic analysis demonstrates CCP and CCP+cECM show**
585 **reduced left ventricular volumes and improved contractile reserve. A-C)**
586 Representative pressure-volume loop recordings of baseline-dobutamine stress from
587 Control, CCP and CCP-cECM treated pigs at 4 weeks following treatment. **D)** LVEF was
588 significantly greater in the CCP group compared to Control. **E)** LVEDV was significantly
589 reduced in CCP and CCP+ECM relative to Control. **F)** LVESV was significantly reduced
590 in CCP and CCPP+ECM groups relative to Control. **G)** End systolic elastance determined
591 from pressure-volume recordings at baseline and after dobutamine show increased
592 contractile reserve in the CCP and CCP+cECM groups.

593 CCP = committed cardiac progenitor cells, cECM = cardiac extracellular matrix, LVEF =
594 left ventricular ejection fraction, LVEDV = left ventricular end diastolic volume, LVESV =
595 left ventricular end systolic volume *p≤0.05, **p≤0.01, ***p≤0.0001

596

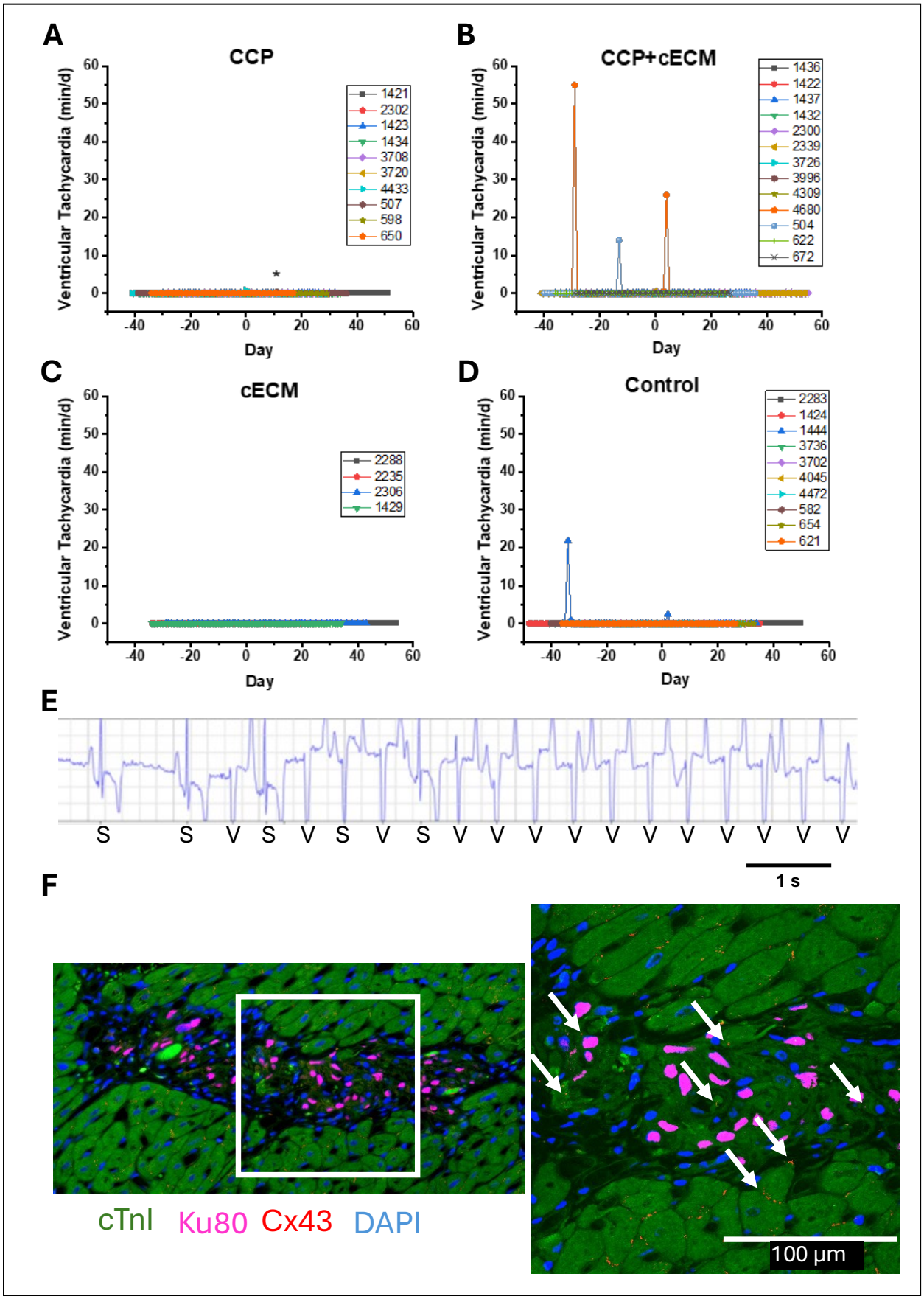

Figure 8. CCP delivery does not result in ventricular tachycardia. A-D) Plots show

598 the daily cumulative time each animal is in ventricular tachycardia (defined as >24 beats
599 at rate >150 bpm) per day for each of the 4 randomized groups with recordings starting
600 the day of MI and day 0 being the day of treatment. **E)** Representative ECG recording of
601 the onset of a 10 s run of ventricular tachycardia detected animal 507 on day 11. S
602 indicates sinus complex and V indicates ventricular complex. CCP = committed cardiac
603 progenitor cells, cECM = cardiac extracellular matrix. **F)** Confocal immunofluorescence
604 image of a graft demonstrating Cx43 labeling within host myocardium, in graft and
605 between graft and host using antibodies to against cTNI, Ku80, and Cx43 with DAPI
606 nuclear labeling. Region in white box is at increased magnification to right.

607 ## REFERENCES

608 1. Tsao CW, Aday AW, Almarzooq ZI, Alonso A, Beaton AZ, Bittencourt MS, Boehme AK, Buxton AE,
609 Carson AP, Commodore-Mensah Y, et al. Heart Disease and Stroke Statistics-2022 Update: A
610 Report From the American Heart Association. *Circulation*. 2022;145:e153-e639. doi:
611 10.1161/CIR.0000000000001052
612 2. Rana JS, Khan SS, Lloyd-Jones DM, Sidney S. Changes in Mortality in Top 10 Causes of Death
613 from 2011 to 2018. *J Gen Intern Med*. 2021;36:2517-2518. doi: 10.1007/s11606-020-06070-z
614 3. Zhang J, Bolli R, Garry DJ, Marban E, Menasche P, Zimmermann WH, Kamp TJ, Wu JC, Dzau VJ.
615 Basic and Translational Research in Cardiac Repair and Regeneration: JACC State-of-the-Art
616 Review. *J Am Coll Cardiol*. 2021;78:2092-2105. doi: 10.1016/j.jacc.2021.09.019
617 4. Riegler J, Tiburcy M, Ebert A, Tzatzalos E, Raaz U, Abilez OJ, Shen Q, Kooreman NG, Neofytou E,
618 Chen VC, et al. Human Engineered Heart Muscles Engraft and Survive Long Term in a Rodent
619 Myocardial Infarction Model. *Circ Res*. 2015;117:720-730. doi: 10.1161/CIRCRESAHA.115.306985
620 5. Laflamme MA, Chen KY, Naumova AV, Muskheli V, Fugate JA, Dupras SK, Reinecke H, Xu C,
621 Hassanipour M, Police S, et al. Cardiomyocytes derived from human embryonic stem cells in pro-
622 survival factors enhance function of infarcted rat hearts. *Nat Biotechnol*. 2007;25:1015-1024.
623 doi: nbt1327 [pii] 10.1038/nbt1327

624 6. Caspi O, Huber I, Kehat I, Habib M, Arbel G, Gepstein A, Yankelson L, Aronson D, Beyar R,
625 Gepstein L. Transplantation of human embryonic stem cell-derived cardiomyocytes improves
626 myocardial performance in infarcted rat hearts. *J Am Coll Cardiol*. 2007;50:1884-1893. doi:
627 10.1016/j.jacc.2007.07.054
628 7. Park SJ, Kim RY, Park BW, Lee S, Choi SW, Park JH, Choi JJ, Kim SW, Jang J, Cho DW, et al. Dual
629 stem cell therapy synergistically improves cardiac function and vascular regeneration following
630 myocardial infarction. *Nature communications*. 2019;10:3123. doi: 10.1038/s41467-019-11091-
631 2
632 8. Weinberger F, Breckwoldt K, Pecha S, Kelly A, Geertz B, Starbatty J, Yorgan T, Cheng KH,
633 Lessmann K, Stolen T, et al. Cardiac repair in guinea pigs with human engineered heart tissue
634 from induced pluripotent stem cells. *Science translational medicine*. 2016;8:363ra148. doi:
635 10.1126/scitranslmed.aaf8781
636 9. Shiba Y, Fernandes S, Zhu WZ, Filice D, Muskheli V, Kim J, Palpant NJ, Gantz J, Moyes KW,
637 Reinecke H, et al. Human ES-cell-derived cardiomyocytes electrically couple and suppress
638 arrhythmias in injured hearts. *Nature*. 2012;489:322-325. doi: 10.1038/nature11317
639 10. Dhahri W, Sadikov Valdman T, Wilkinson D, Pereira E, Ceylan E, Andharia N, Qiang B,
640 Masoudpour H, Wulkan F, Quesnel E, et al. In Vitro Matured Human Pluripotent Stem Cell-
641 Derived Cardiomyocytes Form Grafts With Enhanced Structure and Function in Injured Hearts.
642 *Circulation*. 2022;145:1412-1426. doi: 10.1161/CIRCULATIONAHA.121.053563
643 11. Romagnuolo R, Masoudpour H, Porta-Sanchez A, Qiang B, Barry J, Laskary A, Qi X, Masse S,
644 Magtibay K, Kawajiri H, et al. Human Embryonic Stem Cell-Derived Cardiomyocytes Regenerate
645 the Infarcted Pig Heart but Induce Ventricular Tachyarrhythmias. *Stem cell reports*. 2019;12:967-
646 981. doi: 10.1016/j.stemcr.2019.04.005
647 12. Zhao M, Nakada Y, Wei Y, Bian W, Chu Y, Borovjagin AV, Xie M, Zhu W, Nguyen T, Zhou Y, et al.
648 Cyclin D2 Overexpression Enhances the Efficacy of Human Induced Pluripotent Stem Cell-
649 Derived Cardiomyocytes for Myocardial Repair in a Swine Model of Myocardial Infarction.
650 *Circulation*. 2021;144:210-228. doi: 10.1161/CIRCULATIONAHA.120.049497
651 13. Selvakumar D, Clayton ZE, Prowse A, Dingwall S, Kim SK, Reyes L, George J, Shah H, Chen S,
652 Leung HHL, et al. Cellular heterogeneity of pluripotent stem cell-derived cardiomyocyte grafts is
653 mechanistically linked to treatable arrhythmias. *Nat Cardiovasc Res*. 2024;3:145-165. doi:
654 10.1038/s44161-023-00419-3

655 14. Marchiano S, Nakamura K, Reinecke H, Neidig L, Lai M, Kadota S, Perbellini F, Yang X, Klaiman
656 JM, Blakely LP, et al. Gene editing to prevent ventricular arrhythmias associated with
657 cardiomyocyte cell therapy. *Cell Stem Cell*. 2023;30:396-414 e399. doi:
658 10.1016/j.stem.2023.03.010
659 15. Chong JJ, Yang X, Don CW, Minami E, Liu YW, Weyers JJ, Mahoney WM, Van Biber B, Cook SM,
660 Palpant NJ, et al. Human embryonic-stem-cell-derived cardiomyocytes regenerate non-human
661 primate hearts. *Nature*. 2014;510:273-277. doi: 10.1038/nature13233
662 16. Liu YW, Chen B, Yang X, Fugate JA, Kalucki FA, Futakuchi-Tsuchida A, Couture L, Vogel KW, Astley
663 CA, Baldessari A, et al. Human embryonic stem cell-derived cardiomyocytes restore function in
664 infarcted hearts of non-human primates. *Nat Biotechnol*. 2018;36:597-605. doi:
665 10.1038/nbt.4162
666 17. Shiba Y, Gomibuchi T, Seto T, Wada Y, Ichimura H, Tanaka Y, Ogasawara T, Okada K, Shiba N,
667 Sakamoto K, et al. Allogeneic transplantation of iPS cell-derived cardiomyocytes regenerates
668 primate hearts. *Nature*. 2016;538:388-391. doi: 10.1038/nature19815
669 18. Menasche P, Vanneaux V, Hagege A, Bel A, Cholley B, Parouchev A, Cacciapuoti I, Al-Daccak R,
670 Benhamouda N, Blons H, et al. Transplantation of Human Embryonic Stem Cell-Derived
671 Cardiovascular Progenitors for Severe Ischemic Left Ventricular Dysfunction. *J Am Coll Cardiol*.
672 2018;71:429-438. doi: 10.1016/j.jacc.2017.11.047
673 19. Yap L, Chong LY, Tan C, Adusumalli S, Seow M, Guo J, Cai Z, Loo SJ, Lim E, Tan RS, et al.
674 Pluripotent stem cell-derived committed cardiac progenitors remuscularize damaged ischemic
675 hearts and improve their function in pigs. *NPJ Regen Med*. 2023;8:26. doi: 10.1038/s41536-023-
676 00302-6
677 20. Schmuck EG, Roy S, Dhillon A, Walker S, Spinali K, Colevas S, Zhou T, Chhabra G, Liu Y, Kader
678 Sagar MA, et al. Cultured cardiac fibroblasts and myofibroblasts express Sushi Containing
679 Domain 2 and assemble a unique fibronectin rich matrix. *Exp Cell Res*. 2021;399:112489. doi:
680 10.1016/j.yexcr.2021.112489
681 21. Roy S, Spinali K, Schmuck EG, Kink JA, Hematti P, Raval AN. Cardiac fibroblast derived matrix-
682 educated macrophages express VEGF and IL-6, and recruit mesenchymal stromal cells. *J
683 Immunol Regen Med*. 2020;10. doi: 10.1016/j.regen.2020.100033
684 22. Schmuck EG, Mulligan JD, Ertel RL, Kouris NA, Ogle BM, Raval AN, Saupe KW. Cardiac fibroblast-
685 derived 3D extracellular matrix seeded with mesenchymal stem cells as a novel device to
686 transfer cells to the ischemic myocardium. *Cardiovascular engineering and technology*.
687 2014;5:119-131. doi: 10.1007/s13239-013-0167-1
688 23. Schmuck EG, Hacker TA, Schreier DA, Chesler NC, Wang Z. Beneficial effects of mesenchymal
689 stem cell delivery via a novel cardiac bioscaffold on right ventricles of pulmonary arterial
690 hypertensive rats. *Am J Physiol Heart Circ Physiol*. 2019;316:H1005-H1013. doi:
691 10.1152/ajpheart.00091.2018
692 24. Evseenko D, Zhu Y, Schenke-Layland K, Kuo J, Latour B, Ge S, Scholes J, Dravid G, Li X, MacLellan
693 WR, et al. Mapping the first stages of mesoderm commitment during differentiation of human
694 embryonic stem cells. *Proc Natl Acad Sci U S A*. 2010;107:13742-13747. doi:
695 10.1073/pnas.1002077107
696 25. Kattman SJ, Witty AD, Gagliardi M, Dubois NC, Niapour M, Hotta A, Ellis J, Keller G. Stage-specific
697 optimization of activin/nodal and BMP signaling promotes cardiac differentiation of mouse and
698 human pluripotent stem cell lines. *Cell Stem Cell*. 2011;8:228-240. doi: S1934-5909(10)00703-4
699 [pii] 10.1016/j.stem.2010.12.008

700 26. Zhang J, Tao R, Campbell KF, Carvalho JL, Ruiz EC, Kim GC, Schmuck EG, Raval AN, da Rocha AM,
701 Herron TJ, et al. Functional cardiac fibroblasts derived from human pluripotent stem cells via
702 second heart field progenitors. *Nature communications*. 2019;10:2238. doi: 10.1038/s41467-
703 019-09831-5

704 27. Ivins S, Chappell J, Vernay B, Suntharalingham J, Martineau A, Mohun TJ, Scambler PJ. The
705 CXCL12/CXCR4 Axis Plays a Critical Role in Coronary Artery Development. *Developmental cell*.
706 2015;33:455-468. doi: 10.1016/j.devcel.2015.03.026
707 28. Zhang J, Chu LF, Hou Z, Schwartz MP, Hacker T, Vickerman V, Swanson S, Leng N, Nguyen BK,
708 Elwell A, et al. Functional characterization of human pluripotent stem cell-derived arterial
709 endothelial cells. *Proc Natl Acad Sci U S A*. 2017;114:E6072-E6078. doi:
710 10.1073/pnas.1702295114
711 29. Jebran AF, Seidler T, Tiburcy M, Daskalaki M, Kutschka I, Fujita B, Ensminger S, Bremmer F,
712 Moussavi A, Yang H, et al. Engineered heart muscle allografts for heart repair in primates and
713 humans. *Nature*. 2025;639:503-511. doi: 10.1038/s41586-024-08463-0
714 30. Sultana N, Zhang L, Yan J, Chen J, Cai W, Razzaque S, Jeong D, Sheng W, Bu L, Xu M, et al.
715 Resident c-kit(+) cells in the heart are not cardiac stem cells. *Nature communications*.
716 2015;6:8701. doi: 10.1038/ncomms9701
717 31. van Berlo JH, Kanisicak O, Maillet M, Vagnozzi RJ, Karch J, Lin SC, Middleton RC, Marban E,
718 Molkentin JD. c-kit+ cells minimally contribute cardiomyocytes to the heart. *Nature*.
719 2014;509:337-341. doi: 10.1038/nature13309
720 32. Song H, Yoon C, Kattman SJ, Dengler J, Masse S, Thavaratnam T, Gewarges M, Nanthakumar K,
721 Rubart M, Keller GM, et al. Interrogating functional integration between injected pluripotent
722 stem cell-derived cells and surrogate cardiac tissue. *Proc Natl Acad Sci U S A*. 2010;107:3329-
723 3334. doi: 10.1073/pnas.0905729106
724 33. Fernandes S, Chong JJH, Paige SL, Iwata M, Torok-Storb B, Keller G, Reinecke H, Murry CE.
725 Comparison of Human Embryonic Stem Cell-Derived Cardiomyocytes, Cardiovascular
726 Progenitors, and Bone Marrow Mononuclear Cells for Cardiac Repair. *Stem cell reports*.
727 2015;5:753-762. doi: 10.1016/j.stemcr.2015.09.011
728 34. Blin G, Nury D, Stefanovic S, Neri T, Guillevic O, Brinon B, Bellamy V, Rucker-Martin C, Barbry P,
729 Bel A, et al. A purified population of multipotent cardiovascular progenitors derived from
730 primate pluripotent stem cells engrafts in postmyocardial infarcted nonhuman primates. *J Clin*
731 *Invest*. 2010;120:1125-1139. doi: 40120 [pii]10.1172/JCI40120
732 35. Zhu K, Wu Q, Ni C, Zhang P, Zhong Z, Wu Y, Wang Y, Xu Y, Kong M, Cheng H, et al. Lack of
733 Remuscularization Following Transplantation of Human Embryonic Stem Cell-Derived
734 Cardiovascular Progenitor Cells in Infarcted Nonhuman Primates. *Circ Res*. 2018;122:958-969.
735 doi: 10.1161/CIRCRESAHA.117.311578
736 36. Bellamy V, Vanneaux V, Bel A, Nemetalla H, Emmanuelle Boitard S, Farouz Y, Joanne P, Perier
737 MC, Robidel E, Mandet C, et al. Long-term functional benefits of human embryonic stem cell-
738 derived cardiac progenitors embedded into a fibrin scaffold. *J Heart Lung Transplant*.
739 2015;34:1198-1207. doi: 10.1016/j.healun.2014.10.008
740 37. Poch CM, Foo KS, De Angelis MT, Jennbacken K, Santamaria G, Bahr A, Wang QD, Reiter F,
741 Hornaschewitz N, Zawada D, et al. Migratory and anti-fibrotic programmes define the
742 regenerative potential of human cardiac progenitors. *Nature cell biology*. 2022;24:659-671. doi:
743 10.1038/s41556-022-00899-8
744 38. Nakamura K, Neidig LE, Yang X, Weber GJ, El-Nachef D, Tsuchida H, Dupras S, Kalucki FA,
745 Jayabalu A, Futakuchi-Tsuchida A, et al. Pharmacologic therapy for engraftment arrhythmia
746 induced by transplantation of human cardiomyocytes. *Stem cell reports*. 2021;16:2473-2487.
747 doi: 10.1016/j.stemcr.2021.08.005
748 39. Kawaguchi S, Soma Y, Nakajima K, Kanazawa H, Tohyama S, Tabei R, Hirano A, Handa N, Yamada
749 Y, Okuda S, et al. Intramyocardial Transplantation of Human iPS Cell-Derived Cardiac Spheroids
750 Improves Cardiac Function in Heart Failure Animals. *JACC Basic Transl Sci*. 2021;6:239-254. doi:
751 10.1016/j.jacbts.2020.11.017

752 40. Raval AN, Pepine CJ. Clinical Safety Profile of Transendocardial Catheter Injection Systems: A
753 Plea for Uniform Reporting. *Cardiovasc Revasc Med*. 2021;22:100-108. doi:
754 10.1016/j.carrev.2020.06.031
755 41. Tomkowiak MT, Klein AJ, Vigen KK, Hacker TA, Speidel MA, VanLysel MS, Raval AN. Targeted
756 transendocardial therapeutic delivery guided by MRI-x-ray image fusion. *Catheter Cardiovasc*
757 *Interv*. 2011;78:468-478. doi: 10.1002/ccd.22901
758 42. Raval AN, Cook TD, Duckers HJ, Johnston PV, Traverse JH, Abraham WT, Altman PA, Pepine CJ.
759 The CardiAMP Heart Failure trial: A randomized controlled pivotal trial of high-dose autologous
760 bone marrow mononuclear cells using the CardiAMP cell therapy system in patients with post-
761 myocardial infarction heart failure: Trial rationale and study design. *Am Heart J*. 2018;201:141-
762 148. doi: 10.1016/j.ahj.2018.03.016
763 43. Raval AN, Johnston PV, Duckers HJ, Cook TD, Traverse JH, Altman PA, Dhingra R, Hematti P,
764 Borrello I, Anderson RD, et al. Point of care, bone marrow mononuclear cell therapy in ischemic
765 heart failure patients personalized for cell potency: 12-month feasibility results from CardiAMP
766 heart failure roll-in cohort. *Int J Cardiol*. 2021;326:131-138. doi: 10.1016/j.ijcard.2020.10.043
767 44. Cheng YC, Hsieh ML, Lin CJ, Chang CMC, Huang CY, Puntney R, Wu Moy A, Ting CY, Herr Chan DZ,
768 Nicholson MW, et al. Combined Treatment of Human Induced Pluripotent Stem Cell-Derived
769 Cardiomyocytes and Endothelial Cells Regenerate the Infarcted Heart in Mice and Non-Human
770 Primates. *Circulation*. 2023;148:1395-1409. doi: 10.1161/CIRCULATIONAHA.122.061736
771 45. Zhang H, Xue Y, Pan T, Zhu X, Chong H, Xu C, Fan F, Cao H, Zhang B, Pan J, et al. Epicardial
772 injection of allogeneic human-induced-pluripotent stem cell-derived cardiomyocytes in patients
773 with advanced heart failure: protocol for a phase I/IIa dose-escalation clinical trial. *BMJ Open*.
774 2022;12:e056264. doi: 10.1136/bmjopen-2021-056264

775